JCI insight

Homozygous loss-of-function mutations in *SLC26A7* cause goitrous congenital hypothyroidism

Hakan Cangul, … , Samuel Refetoff, Nadia Schoenmakers

JCI Insight. 2018;3(20):e99631. https://doi.org/10.1172/jci.insight.99631.

Research Article | Endocrinology | Genetics

Defects in genes mediating thyroid hormone biosynthesis result in dyshormonogenic congenital hypothyroidism (CH). Here, we report homozygous truncating mutations in *SLC26A7* in 6 unrelated families with goitrous CH and show that goitrous hypothyroidism also occurs in *Slc26a7*-null mice. In both species, the gene is expressed predominantly in the thyroid gland, and loss of function is associated with impaired availability of iodine for thyroid hormone synthesis, partially corrected in mice by iodine supplementation. *SLC26A7* is a member of the same transporter family as *SLC26A4* (pendrin), an anion exchanger with affinity for iodide and chloride (among others), whose gene mutations cause congenital deafness and dyshormonogenic goiter. However, in contrast to pendrin, SLC26A7 does not mediate cellular iodide efflux and hearing in affected individuals is normal. We delineate a hitherto unrecognized role for SLC26A7 in thyroid hormone biosynthesis, for which the mechanism remains unclear.

Find the latest version:

http://jci.me/99631/pdf

JCI insight

RESEARCH ARTICLE

Homozygous loss-of-function mutations in *SLC26A7* cause goitrous congenital hypothyroidism

Hakan Cangul,[1] Xiao-Hui Liao,[2] Erik Schoenmakers,[3] Jukka Kero,[4,5] Sharon Barone,[6] Panudda Srichomkwun,[2] Hideyuki Iwayama,[2] Eva G. Serra,[7] Halil Saglam,[8] Erdal Eren,[8] Omer Tarim,[8] Adeline K. Nicholas,[3] Ilona Zvetkova,[3] Carl A. Anderson,[7] Fiona E. Karet Frankl,[9] Kristien Boelaert,[10] Marja Ojaniemi,[11] Jarmo Jääskeläinen,[12] Konrad Patyra,[4] Christoffer Löf,[4] E. Dillwyn Williams,[13] UK10K Consortium,[14] Manoocher Soleimani,[6] Timothy Barrett,[15] Eamonn R. Maher,[16] V. Krishna Chatterjee,[3] Samuel Refetoff,[2,17] and Nadia Schoenmakers[3]

[1]Department of Medical Genetics, Istanbul Medipol University, International School of Medicine, Istanbul, Turkey. [2]Department of Medicine, The University of Chicago, Chicago, Illinois, USA. [3]Metabolic Research Laboratories, Wellcome Trust-Medical Research Council Institute of Metabolic Science, Addenbrooke's Hospital, University of Cambridge, Cambridge, United Kingdom (UK). [4]Research Centre for Integrative Physiology and Pharmacology, Institute of Biomedicine, University of Turku, Turku, Finland [5]Department of Paediatrics, Turku University Hospital, Turku, Finland. [6]University of Cincinnati and Veterans Administration Hospital, Cincinnati, Ohio, USA. [7]Department of Human Genetics, The Wellcome Trust Sanger Institute, Hinxton, Cambridge, UK. [8]Uludag University School of Medicine, Department of Paediatric Endocrinology, Bursa, Turkey. [9]Department of Medical Genetics and Division of Renal Medicine, University of Cambridge, Cambridge, UK. [10]Institute of Metabolism and Systems Research, University of Birmingham and Centre for Endocrinology, Diabetes and Metabolism, Birmingham Health Partners, Edgbaston, Birmingham, UK. [11]PEDEGO Research Center and MRC Oulu, University of Oulu, and Department of Children and Adolescents, Oulu University Hospital, Oulu, Finland. [12]Department of Pediatrics, University of Eastern Finland and Kuopio University, Hospital, Kuopio, Finland. [13]Thyroid Carcinogenesis Group, University of Cambridge, Strangeways Research Laboratory, Cambridge, UK. [14]The UK10K Consortium detailed in the Supplemental Acknowledgments. [15]Institute of Cancer and Genomic Sciences, College of Medical and Dental Sciences, University of Birmingham and Department of Endocrinology, Birmingham Children's Hospital, Birmingham, UK. [16]Department of Medical Genetics, University of Cambridge and NIHR Cambridge Biomedical Research Centre, Cambridge, UK. [17]Department of Pediatrics and the Committee on Genetics, The University of Chicago, Chicago, Illinois, USA.

Defects in genes mediating thyroid hormone biosynthesis result in dyshormonogenic congenital hypothyroidism (CH). Here, we report homozygous truncating mutations in *SLC26A7* in 6 unrelated families with goitrous CH and show that goitrous hypothyroidism also occurs in *Slc26a7*-null mice. In both species, the gene is expressed predominantly in the thyroid gland, and loss of function is associated with impaired availability of iodine for thyroid hormone synthesis, partially corrected in mice by iodine supplementation. *SLC26A7* is a member of the same transporter family as *SLC26A4* (pendrin), an anion exchanger with affinity for iodide and chloride (among others), whose gene mutations cause congenital deafness and dyshormonogenic goiter. However, in contrast to pendrin, SLC26A7 does not mediate cellular iodide efflux and hearing in affected individuals is normal. We delineate a hitherto unrecognized role for SLC26A7 in thyroid hormone biosynthesis, for which the mechanism remains unclear.

Authorship note: HC and XHL contributed equally to this work.

Conflict of interest: The authors have declared that no conflict of interest exists

License: This work is licensed under the Creative Commons Attribution 4.0 International License. To view a copy of this license, visit http://creativecommons.org/licenses/by/4.0/.

Submitted: January 4, 2018
Accepted: September 6, 2018
Published: October 18, 2018

Reference information:
JCI Insight. 2018;3(20):e99631. https://doi.org/10.1172/jci.insight.99631.

Introduction

Congenital hypothyroidism (CH), the commonest neonatal endocrine disorder, is caused by either maldevelopment of the gland (dysgenesis) or failure of hormone biosynthesis in a structurally intact gland (dyshormonogenesis). As thyroid hormone is indispensable for neurological development, growth, and metabolic homeostasis in childhood, delayed diagnosis and treatment of CH results in profound neurodevelopmental and growth retardation. Accordingly, screening programs operate in most countries to facilitate prompt neonatal diagnosis (1).

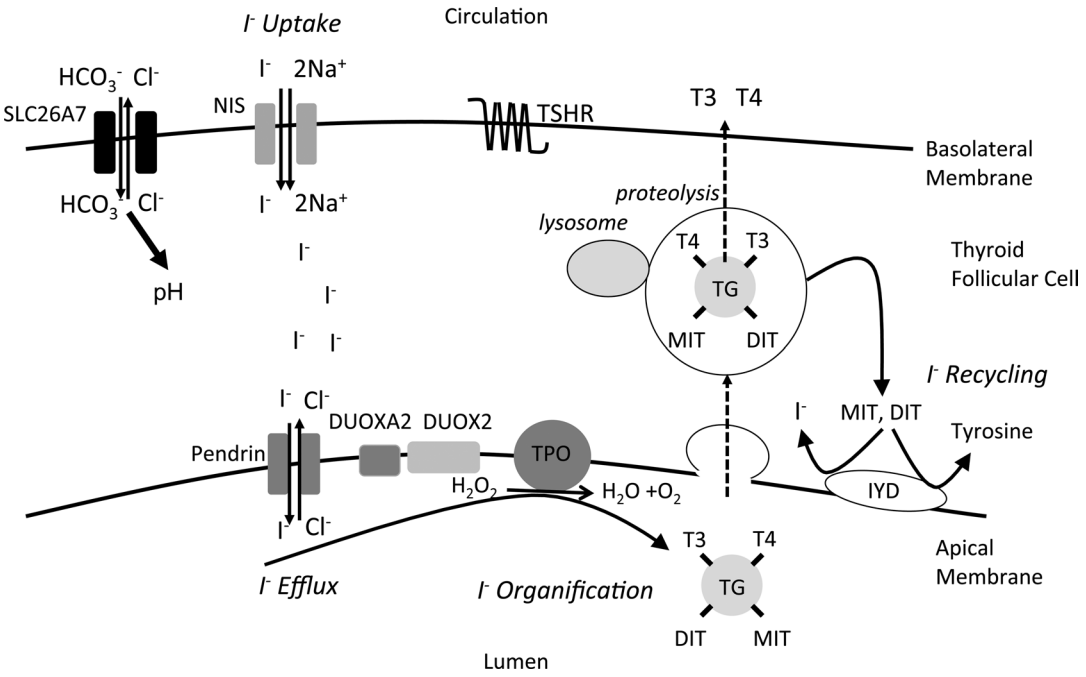

Figure 1. Thyroid hormone biosynthesis pathway. Schematic depicting the thyroid follicular cell and key components of the thyroid hormone biosynthesis pathway. The major steps in iodide metabolism (uptake, efflux, organification, and recycling) are shown. In murine thyroid, Slc26a7 localizes intracellularly and to the basal membrane; given its known function as a chloride-bicarbonate transporter in other cell types, Slc26a7 may alter intracellular pH, thereby altering iodide uptake or iodide organification as we have observed in murine or human contexts, respectively. DIT, diiodothyronine; MIT, monoiodothyronine.

Recent reports indicate that CH occurs primarily in association with a eutopic, normal-sized thyroid gland, suggesting that dyshormonogenic etiologies may be more important than previously anticipated (2). Thyroid hormonogenesis requires sufficient iodide substrate, in addition to an intact molecular pathway including enzymes, transporter molecules, and thyroglobulin (TG). Active uptake of iodide across the thyrocyte basolateral membrane is mediated by the sodium-iodide symporter (NIS). Iodide is then transported across the apical membrane, facilitated, at least in part, by pendrin, acting as a chloride-iodide exchanger. Iodide is then oxidized and incorporated into tyrosyl residues of TG. Such organification of iodide is catalyzed by thyroid peroxidase (TPO) and requires H_2O_2 generated by dual oxidase type 2 (DUOX2) and its accessory protein DUOXA2. Unused iodotyrosines are subsequently deiodinated by iodotyrosine dehalogenase (IYD) enabling recycling of intrathyroidal iodide (Figure 1). Mutations in known thyroid biosynthetic pathway genes are identified frequently in dyshormonogenic CH, with patient phenotypes validating the importance of these proteins in thyroid hormonogenesis (1). We hypothesized that genetic analyses of cases lacking pathogenic mutations in known genes might identify novel etiologies of dyshormonogenesis. Here, in kindreds lacking mutations in known causative genes, we describe human cases with goitrous, dyshormonogenic CH due to homozygous mutations in SLC26A7, an anion transporter, previously shown to function as a chloride-bicarbonate exchanger or chloride channel, mediating murine renal bicarbonate resorption and gastric acid secretion (3). Additionally, we delineate a homologous, goitrous hypothyroid phenotype in *Slc26a7*-null mice.

Results

Clinical cases. Six families harboring *SLC26A7* mutations were studied. Families A, B, and C were consanguineous and of Pakistani (A and B), or Turkish (C) origin. Families D, E, and F were Finnish non-consanguineous kindreds. All children were found to have CH by neonatal screening except for patients of family C, who presented with symptomatic hypothyroidism at 3 weeks of age, since CH screening was not available at the site of their birth. All 13 affected individuals had moderate to severe primary CH as defined by European Society for Paediatric Endocrinology (ESPE) criteria (4), with goiter in 8 cases. Less marked neonatal thyroid-stimulating hormone (TSH) elevation in AII.iv and AII.v born at 33 weeks, may reflect immaturity of their hypothalamic-pituitary-thyroid axes (Figure 2A) since withdrawal of levothyroxine

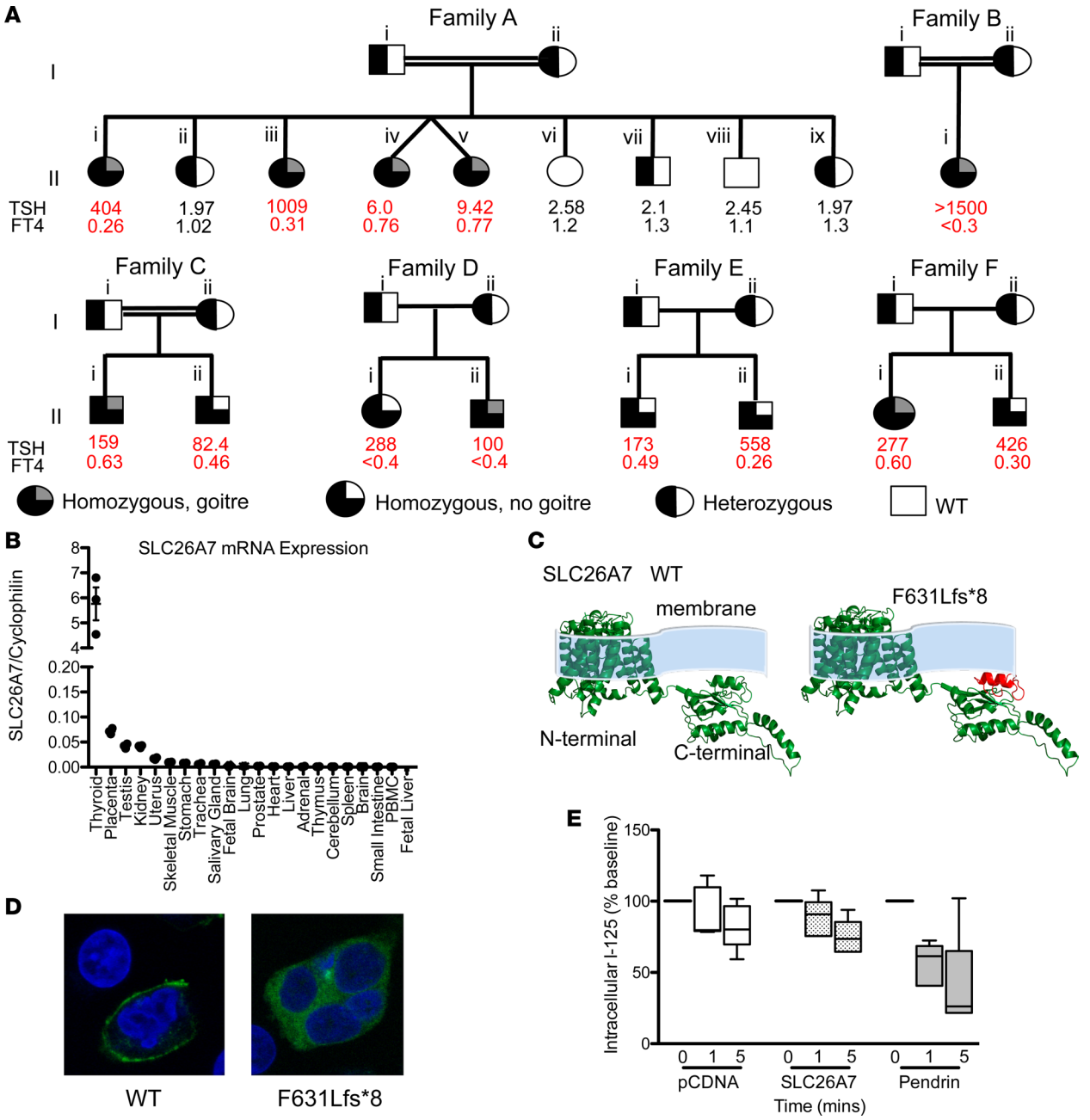

Figure 2. Clinical genotype and phenotype data for kindreds harboring SLC26A7 mutations, and functional characterization of wild-type and mutant SLC26A7. (**A**) Pedigrees of 6 kindreds illustrating cases with congenital hypothyroidism (CH) and unaffected relatives for whom genetic data were available. Thyroid hormone measurements refer to venous measurements made at diagnosis of CH or following genetic evaluation. Reference ranges: AII.i, iii, iv, v thyroid-stimulating hormone (TSH) 0.9–3.5 mU/l, free thyroxine (FT4) 1.1–1.8 ng/dl; AII.ii TSH 0.6–4.8 mU/l, FT4 0.76–1.5 ng/dl; AII.vi. vii, viii, ix TSH 0.4–3.5 mU/l, FT4 0.83–1.69 ng/dl; BII.i TSH 0.7–5.3 mU/l, FT4 1.1–1.8 ng/dl; CII.i TSH 0.6–4.8 mU/l, FT4 0.8–1.5 ng/dl; CII.ii TSH 0.4–3.5 mU/l, FT4 0.8–1.9 ng/dl; DII.i, ii, EII.i, ii, FII.i, ii TSH 0.35–40 mU/l, FT4 0.7–1.5 ng/dl. Double horizontal lines indicate consanguinity. FT4: multiply by 12.87 to convert to pmol/l. (**B**) Quantitative RT-PCR analysis of SLC26A7 mRNA expression in a human tissue library relative to cyclophilin; horizontal bars denote mean and vertical bars standard error of the mean. (**C**) Homology modeling predicting the protein consequences of the SLC26A7 p.F631Lfs*8 mutation. The deleted protein region is shown in red. (**D**) HEK293 cells transfected with GFP-tagged wild-type and F631Lfs*8 SLC26A7 demonstrate localization of wild-type protein to the plasma membrane, whereas the mutant remains intracellular (total original magnification, ×63). (**E**) Box-and-whisker plots for time-dependent iodide efflux from HEK293 cells cotransfected with NIS and pCDNA (white), pendrin (gray), or SLC26A7 (stippled black); $n = 5$ experiments. Boxes extend from the 25th to 75th percentiles, the horizontal line represents the median, and the vertical bars represent the minimum and maximum values.

treatment in AII.v age 9.8 years suggested permanent hypothyroidism: high TSH of 142 mU/l, low free thyroxine (FT4) <0.3 ng/dl (<3.9 pmol/l), and free triiodothyronine (FT3) of 0.33 ng/dl (5.0 pmol/l).

AII.i was noted clinically to have a moderately large goiter (age 5 years), which persisted throughout childhood. Ultrasonography (age 10 years), showed an enlarged, heterogeneous, hypervascular thyroid, with

Table 1. Serum biochemistry, thyroid radioiodine uptake, and perchlorate discharge test results in cases with homozygous *SLC26A7* mutations

Case	Age (years)	TG (μg/l)	TSH (mU/l)	FT4 (ng/dl)[A]	FT3 (ng/dl)[B]	% I^- uptake 5%–25% (2 hr)	Perchlorate discharge (%)
AII.i	12.7	**358.5** (1–35)	**22.6** (0.6-4.8)	**0.63** (0.76-1.49)	0.53 (0.23-0.55)	**20**	**38.5**
AII.iii	9.3	**386** (1–35)	**15.9** (0.4–3.5)	0.89 (0.83–1.69)	**0.61** (0.23–0.55)	**36**	**14.5**
BII.i	3	NA	**131** (0.4–3.5)	**<0.30** (0.83–1.69)	NA	NA	**47**[C]
CII.i	5.7	**320** (1.6–60)	**7.6** (0.35–4.9)	1.22 (0.7–1.48)	**0.52** (0.17–0.37)	**50**	**39**

Serum biochemistry, thyroid radioiodine (I) uptake, and perchlorate discharge test results in cases with homozygous *SLC26A7* mutations. Levothyroxine was omitted for 3 weeks prior to evaluation. Discharge of 10%–79% following perchlorate was defined as a partial iodide organification defect. [A]Multiply by 12.87 to convert FT4 to pmol/l. [B]Multiply by 15.4 to convert FT3 to pmol/l. [C]Based on 15% thyroidal uptake at 30 minutes. FT3, free triiodothyronine; FT4, free thyroxine; TG, thyroglobulin; TSH, thyroid-stimulating hormone. Numbers in parentheses indicate the reference ranges. Bold numbers are values outside the reference range.

numerous focal cysts; at age 14.5 years thyroid volume measured 68 ml. AII.iii developed goiter at age 3.6 years, with a large goiter evident clinically (volume 91 ml) at age 11 years. Due to poor compliance with thyroxine therapy, TSH levels were frequently elevated in both children. Small goiters were evident clinically in AII.iv and AII.v (age 1 month), with raised TSH levels (11 and 37 mU/l, respectively) and increased thyroid volumes (24.4 ml and 44.4 ml on ultrasound, respectively) at 9.8 years of age. A small goiter was noted clinically following thyroxine withdrawal in BII.i at age 3 years and in CII.i at age 5.7 years, with progressive enlargement in the latter. FII.i and DII.ii exhibited a large goiter at birth that persisted in FII.i but resolved in DII.ii (ultrasound dimensions at birth: FII.i, right lobe anterior-posterior diameter 31 mm, left lobe 27 mm; DII.ii, right thickness 16 mm, left 14 mm). Although the mother of FII.i had autoimmune hypothyroidism, she was adequately replaced with levothyroxine during pregnancy. CII.ii, FII.ii, DII.i, and the siblings in family E did not exhibit goiter.

Perchlorate discharge tests were performed in 4 cases following cessation of levothyroxine treatment for 3 to 4 weeks, and showed partial iodide organification defects (PIODs). The mean perchlorate-induced iodide discharge was 35%, range 14.5%–47% (normal <10%, PIOD 10%–79%), with elevated or high-normal early (2 hour) thyroidal radioiodine uptake (mean 35%, range 20%–50%, reference range [RR] 5%–25%). Concurrent biochemical measurements showed elevated TG and elevated or high-normal FT3 levels (Table 1).

Genetic studies. Whole exome sequencing (WES) in kindreds A, D, and E and subsequent Sanger sequencing in kindreds B, C, and D identified biallelic truncating mutations in *SLC26A7* in all affected individuals (c.679C>T, p.R227* families A, B, and C; c.1893delT, p.F631Lfs*8 families D, E, and F). All affected individuals were homozygous for the mutations (Figure 2A), which were rare with minor allele frequencies 0.00001653 (p.R227*) and 0.0002974 (p.F631Lfs*8), with no reported homozygous cases in the Exome Aggregation Consortium (ExAC; http://exac.broadinstitute.org, accessed October 2017). There are also no biallelic truncating variants (nonsense or frameshift) in *SLC26A7* in the ExAC database, suggesting this type of mutational event is exceptionally rare in the general population. Heterozygous carriers of *SLC26A7* mutations were euthyroid with the exception of DI.i, age 48 years, who exhibited subclinical hypothyroidism and F1.i who at age 29 years was diagnosed with autoimmune hypothyroidism (Supplemental Tables 1 and 2; supplemental material available online with this article; https://doi.org/10.1172/jci.insight.99631DS1).

SLC26A7 expression studies and functional characterization. Expression profiling of different human tissues showed strong predominance of the *SLC26A7* transcript in thyroid, suggesting a physiological role (Figure 2B). This is corroborated in the Genotype Tissue Expression portal, (https://www.gtexportal.org/home/gene/SLC26A7), with SLC26A7 demonstrating a clear overexpression in thyroid tissue. Differential splicing at the human *SLC26A7* locus generates 2 different full-length protein isoforms (variant 1, 656 amino acids, NP_439897; variant 2, 663 amino acids, NP_599028). Isoform-specific quantitative reverse transcriptase PCR (qPCR) showed minimal thyroidal expression of variant 2 (data not shown), so functional studies were undertaken in a variant 1 background.

SLC26A7 c.679C>T terminates its mRNA transcript very prematurely (ENST00000276609.7, R227*; 1,257 nt before the last exon junction), strongly predicting its nonsense-mediated decay (5), but undetectable *SLC26A7* mRNA expression in peripheral blood mononuclear cells (PBMCs; see Figure 2B) precluded validation using blood samples. *SLC26A7* c.1893delT is predicted to produce a truncated protein more distally (p.F631Lfs*8). Homology modeling suggested destabilization of its carboxyterminal sulfate transporter and antisigma factor antagonist (STAS) domain, which is required for membrane localization and exchanger function (6) (Figure 2C). Consistent with this, wild-type GFP-tagged SLC26A7 localized to the membrane in transfected cells, whereas the p.F631Lfs*8-SLC26A7 mutant remained intracellular (Figure 2D).

As SLC26A7 is homologous to pendrin (SLC26A4) and humans homozygous for *SLC26A7* mutations exhibit impaired iodide organification, we hypothesized that SLC26A7 might mediate apical iodide transport in the thyrocyte. However, in contrast to increased iodine efflux from cells expressing pendrin, radioiodine loss from SLC26A7-expressing cells was not enhanced, being comparable to control, mock-transfected cells (Figure 2E). Furthermore, in contrast to sensorineural deafness in pendrin deficiency, hearing in our patients was normal.

Dyshormonogenic hypothyroidism in Slc26a7-null mice. *Slc26a7*-null mice exhibit perturbed acid-base homeostasis, with distal renal tubular acidosis and impaired gastric acid production (3). Accordingly, we investigated acid-base status in our patients, but all individuals homozygous for *SLC26A7* mutations showed normal serum electrolytes and renal function (Supplemental Table 3), with no clinical evidence of achlorhydria. Recent data also support a role for rodent Slc26a7 in dental enamel formation (7); however, our patients did not exhibit abnormal dentition.

Having documented hypothyroidism in humans with defective SLC26A7, we evaluated the *Slc26a7*-null mice, whose thyroid status had not been previously investigated. *Slc26a7*-null male mice showed hypothyroidism, with low serum T4 levels when first tested at day 14 postpartum (P14) and significantly elevated serum TSH, and low T4 and T3 levels thereafter (Figure 3A). Hypothyroidism was recapitulated in both sexes; furthermore, there was no difference in thyroid status between heterozygous mice and wild-type animals (Supplemental Figure 1, A and B). Similar to human thyroid, *Slc26a7* mRNA is predominantly expressed in murine thyroid (Figure 3B). Goiter was evident from P14 onwards, with 1.7-fold increased thyroid weight in homozygous compared with wild-type animals and 21.5-fold greater at P90. Thyroid histology from homozygous *Slc26a7*-null mice showed enlarged follicles with excess colloid lined by normal or tall follicular epithelium (Figure 3, C and D).

We found that available anti-SLC26A7 sera could not reliably localize SLC26A7 protein in human or murine thyroid. Accordingly, we undertook thyroid immunohistochemistry in a different transgenic mouse line expressing FLAG-epitope-tagged Slc26a7 (architecture of modified gene locus and genotype data summarized in Supplemental Figure 2). Anti-FLAG immunostaining in male Slc26a7-FLAG homozygotes showed predominantly intracellular protein, with more marked expression at or immediately adjacent to the basal membrane (Figure 3E).

Additional studies in *Slc26a7*-null mice sought to characterize the nature of defective thyroid hormone biosynthesis. Decreased intrathyroidal concentrations of both TG-bound and free thyroid hormones in null mice suggested defective TG iodination and thyroid hormone biosynthesis rather than impaired secretion (Figure 4). In contrast to humans, radioiodine studies in null mice showed reduced tracer uptake with normal discharge following perchlorate administration (Supplemental Figure 1, C and D). However, studies in HEK293 cells transfected with SLC26A7, either alone or coexpressed with SLC5A5 (NIS), did not show altered iodide uptake (Supplemental Figure 3A).

Supplementation of 30 μg iodide/day, or 40-fold the minimum required amount (7-fold higher than that in regular mouse chow), to *Slc26a7*-null male mice partially reversed the hypothyroidism, achieving an exponential decline in TSH ($P < 0.001$, 1-way ANOVA) and increase in T3 levels ($P < 0.05$, 2-way ANOVA) not seen in heterozygous controls. After 6 weeks of treatment, TSH and T3 concentrations in *Slc26a7*-null and euthyroid, heterozygous mice were comparable; however, T4 levels did not change during the treatment. In keeping with amelioration of biochemical hypothyroidism, KI treatment of *Slc26a7*-null mice produced a significant increase in body weight, consistent with increased growth ($P < 0.001$, 1-way ANOVA). Serum iodide concentrations increased significantly in both heterozygous and *Slc26a7*-null mice with KI supplementation ($P < 0.001$, 2-way ANOVA). However, both baseline and post-supplementation serum iodide levels were most markedly elevated in null mice ($P < 0.005$) (Supplemental Figure 3, B–F). This is consistent with reduced thyroidal iodide uptake, although impaired renal excretion cannot be excluded.

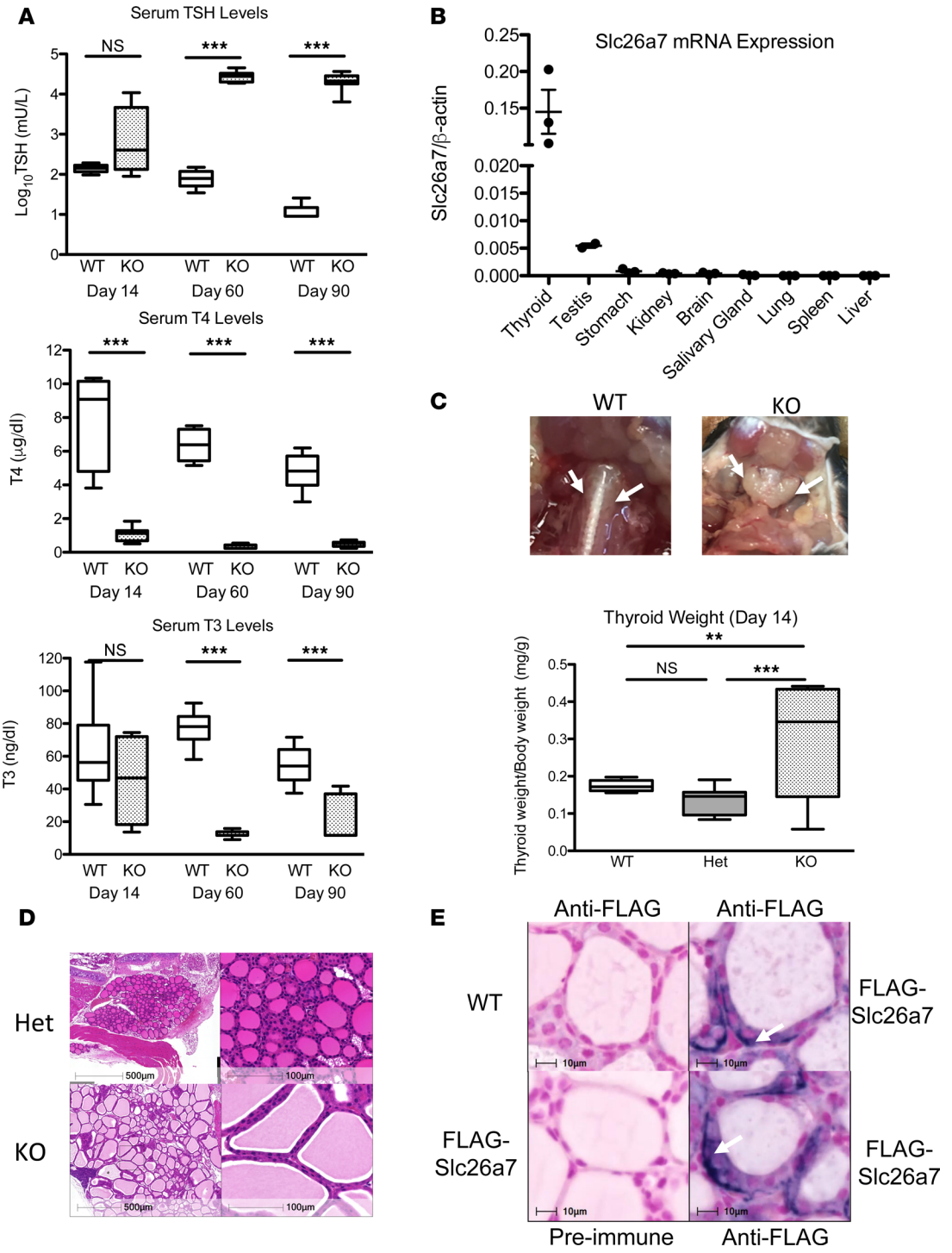

Figure 3. Characterization of the thyroid phenotype in *Slc26a7*-null mice and evaluation of murine thyroidal Slc26a7 expression. (**A**) Box-and-whisker plots for log_{10}TSH, T4, and T3 measurements in male wild-type (WT, white), and *Slc26a7*-null mice (KO, stippled black) at 14, 60, and 90 days of age; n = 6–12 mice of each genotype. Boxes extend from the 25th to 75th percentiles, the horizontal line represents the median, and the vertical bars represent the minimum and maximum values. P values were calculated using an unpaired 2-tailed Student's t test. ***$P < 0.0005$. (**B**) Quantitative RT-PCR analysis of Slc26a7 mRNA expression in a murine tissue library relative to cyclophilin. Horizontal bars represent the mean and error bars represent the standard error of the mean. (**C**) Photographic representation of the thyroid gland in a male wild-type and *Slc26a7*-null mouse age 90 days, demonstrating goiter in the *Slc26a7*-null mouse. Box-and-whisker plots below quantify mean thyroid weight/body weight in 5 WT (white), 18 heterozygous (Het, gray), and 8 *Slc26a7*-null male mice (KO, stippled black) at P14. P values were calculated using 1-way ANOVA with the Newman-Keuls multiple-comparisons test. **$P < 0.005$, ***$P < 0.0005$. (**D**) Hematoxylin and eosin–stained thyroid sections from a male *Slc26a7*-null (KO) mouse compared with a heterozygous littermate (Het) as control age 60 days. Images are representative of sections reviewed from 3 separate goitrous mice and demonstrate enlarged, colloid-filled follicles with normal-tall follicular cells. Scale bars: 500 μm (top left) and 100 μm. (**E**) Representative thyroid sections from 2 different Slc26a7-FLAG male mice and a wild-type mouse age 75 days, stained with anti-FLAG antibody or preimmune serum (control). Arrows denote intracellular and basolateral localization of SLC26A7. Scale bars: 10 μm. NS, not significant.

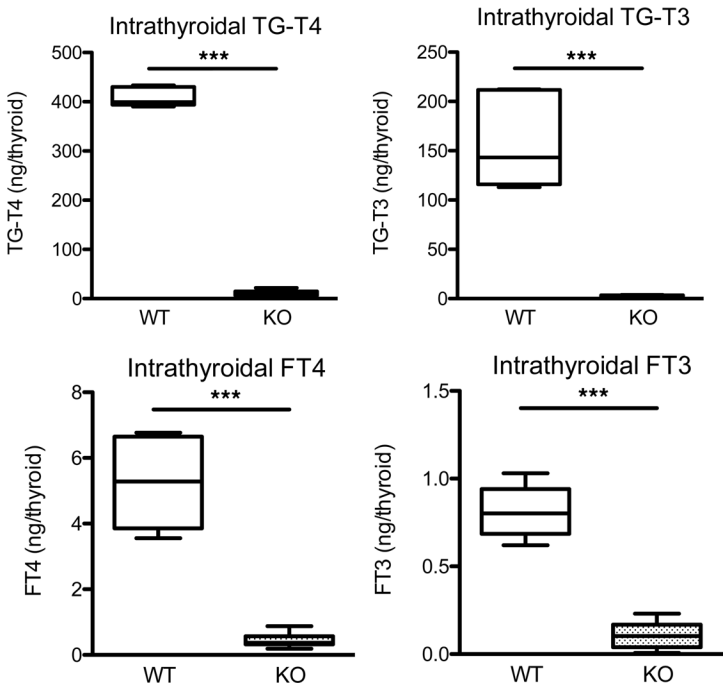

Figure 4. Intrathyroidal hormone measurements in male *Slc26a7*-null mice. Box-and-whisker plots for intrathyroidal TG-bound and free (F) T4 and T3 levels in male wild-type (WT, white) and homozygous *Slc26a7*-null mice (KO, stippled black) age 90 days. Boxes extend from the 25th to 75th percentiles, the horizontal line represents the median, and the vertical bars represent the minimum and maximum values. Measurements were made from 6–10 mice of each genotype. *P* values were calculated using an unpaired 2-tailed Student's *t* test. ***$P < 0.0005$.

Discussion

Our studies indicate that SLC26A7 is indispensable for thyroid hormone biosynthesis in humans and mice. In both species, SLC26A7 is predominantly expressed in the thyroid gland, with disruption of its function resulting in goitrous CH. A greater reduction of T4 than T3, together with a partial iodide organification defect in humans with homozygous *SLC26A7* defects is consistent with reduced TG iodination leading to dyshormonogenesis. Indeed, since the first submission of this report, biallelic, truncating mutations in SLC26A7 were reported in a single Saudi Arabian family with dyshormonogenetic CH (8). Due to differing dietary iodine intake, variable TSH levels in utero, genetic background, and other unknown factors, variability of goiter (presence and size) is recognized in dyshormonogenesis despite identical genetic basis (9). *Slc26a7*-null mice exhibit a homologous phenotype of early postnatal hypothyroidism, with enlarged thyroid gland and more severely reduced T4 than T3 in serum and in thyroid, both indicating impaired iodine availability for hormone biosynthesis.

Our identification of *SLC26A7* mutations in dyshormonogenic CH widens the known spectrum of human disease associated with the 10-member SLC26 anion transporter and channel protein family: *SLC26A2* sulfate transporter mutations disrupt proteoglycan sulfation resulting in a spectrum of chondrodysplasias; defects in *SLC26A3*, a colonic Cl^-/HCO_3^- exchanger, cause congenital, chloride-losing diarrhea; *SLC26A4* mutations causing deficiency in pendrin, an apical iodide transporter in thyroid cells and Cl^-/HCO_3^- exchanger in the cochlear endolymphatic system, result in congenital deafness and dyshormonogenic goiter (10).

Although SLC26A7 shares substantial homology with pendrin, SLC26A7-related CH is clinically distinct from the phenotype associated with loss of pendrin function and our data do not support a direct role for SLC26A7 in mediating cellular iodide efflux. Indeed, whilst the existence of additional transporters other than pendrin mediating iodide efflux from the thyrocyte are long recognized, recent studies suggest that anoctamin-1 may fulfil this function, although the relative physiological roles of these proteins requires further evaluation (11, 12).

SLC26A7 function was previously characterized in rodents, where it maintains acid-base homeostasis by facilitating renal bicarbonate resorption via Cl^-/HCO_3^- exchange at the basolateral membrane of the α-intercalated cells in the outer medullary collecting duct (OMCD) (13). It also localizes to the basolateral

membrane of gastric parietal cells and may either facilitate HCO_3^- efflux or function as a Cl^- channel, regulating gastric acid secretion (14, 15, 3) in agreement with our localization of Slc26a7 protein to both intracellular and basal membrane compartments in thyroid follicular cells. Additionally, Slc26a7 contributes to maintenance of the pH regulatory network during maturation of murine tooth enamel (7). With documented distal renal tubular acidosis and gastric achlorhydria in *Slc26a7*-null mice, we found no overt renal acid-base abnormalities in our homozygous *SLC26A7*-mutant patients in the healthy state, but cannot exclude its role when homeostasis is perturbed, analogous to the renal role of pendrin during systemic metabolic alkalosis (16).

The precise mechanism by which SLC26A7 regulates murine and human thyroid hormone biosynthesis requires further investigation. In humans, defective SLC26A7 results in impaired iodide organification with preserved thyroidal iodide uptake; however, in vitro studies did not demonstrate a direct role for SLC26A7 in mediating iodide efflux. Slc26a7 expression at the basolateral membrane in murine thyrocytes, and impaired iodide uptake with partial reversal of hypothyroidism after iodide supplementation in *Slc26a7*-null mice, suggest a role for Slc26a7 in thyroidal uptake of iodide. However, in both mice and humans, the sodium-iodide transporter (NIS/SLC5A5) is the major mediator of thyroidal iodide uptake, with loss of SLC5A5 function resulting in profound CH in both species (17, 18), suggesting a permissive rather than direct role for Slc26a7 in facilitating iodide uptake in mice. Furthermore, preserved thyroidal iodide uptake in SLC26A7-deficient humans suggests that Slc26a7 transporter function may differ between the two species. A precedent for this is provided by the observation that the KCNQ1-KCNE2 potassium channel is crucial in facilitating murine NIS activity, whereas biallelic KCNQ1 mutations in humans predispose to cardiac arrhythmias but not thyroid dysfunction (19, 20).

The role of SLC26A7 as a Cl^-/HCO_3^- exchanger, controlling acid-base balance in the renal tubule and gastric epithelium, may indicate an analogous function in thyroid follicular cells, since optimal ionic milieu and pH are known to be critical for enzyme (TPO, DUOX2) and anion exchanger activities during thyroid hormone biosynthesis (21). It is therefore possible that SLC26A7 plays a common role in thyroidal Cl^-/HCO_3^- homeostasis in humans and mice, with species differences in thyroid cell electrophysiology mediating divergent effects on iodide metabolism, perhaps accounting for the preserved iodide uptake but impaired organification we observed in human SLC26A7 deficiency, with reduced iodide uptake and normal organification in *Slc26a7*-null mice (Figure 1). Future research aims to map the subcellular location of Slc26a7 in thyrocytes from both species more precisely and measure intracellular pH, changes in ionic milieu, and function of proteins mediating iodide uptake, efflux, and organification in wild-type or mutant-Slc26a7-expressing cells.

We have identified what we believe is a novel genetic cause of dyshormonogenic CH, and delineated a critical role for SLC26A7 in human and murine thyroid hormone biosynthesis. Although there are notable differences in the effect of SLC26A7 deficiency in humans and mice, such as thyroidal uptake, perchlorate discharge, and the effect on kidneys and teeth, both species manifest congenital goitrous hypothyroidism. Further, irrespective of the precise mechanism of SLC26A7 action, in both species thyroid hormone deficiency is caused by reduction of iodine availability for hormone synthesis. Both humans and mice have more severe reduction of T4 than T3 in thyroid as well as in serum at baseline and this is partially corrected by iodide supplementation in the mouse. An increase in the T3 to T4 ratio has been observed in endemic areas of iodine deficiency as well as in reduced iodine uptake due to NIS defects (17). It reflects the relative abundance of monoiodotyrosine due to poor iodination of TG with the consequent predominant synthesis of T3 rather than T4.

Methods

Case selection. Cases with CH and eutopic gland-in-situ, in whom mutations in known dyshormonogenesis-associated genes had been excluded, were recruited.

Genetic studies. WES of genomic DNA samples was used to identify rare, biallelic variants in genes with a likely role in thyroid physiology, which segregated with disease within and across families. The index cases (AII.i, AII.iii) were sequenced under the auspices of the UK10K project, www.UK10K.org (22). Sanger sequencing was used to verify WES findings and to identify additional cases harboring *SLC26A7* gene mutations (detailed methods are available in the supplemental section). Next-generation sequence data that support this study have been deposited in the European Genome-phenome Archive (EGA) under the data set accession codes EGAD00001000420 and EGAD00001004293.

In silico modeling. The model for SLC26A7 was generated using the phyre2 (Protein Homology/AnalogY Recognition Engine 2) web portal, which predicts and analyzes protein structures based on

homology/analogy recognition to solved protein crystal structures (23). The figures were generated with MacPyMOL Molecular Graphics System, Schrödinger, LLC.

Expression of SLC26A7. SLC26A7 mRNA expression was measured in human and murine tissue RNA libraries using qPCR. The Slc26a7 protein expression pattern was evaluated immunohistochemically in transgenic mice expressing FLAG-epitope-tagged Slc26a7 (see Methods section and supplemental appendix).

Cellular localization of SLC26A7 and iodide transport studies. Expression vectors containing GFP-tagged wild-type or mutant SLC26A7 complementary DNAs or wild-type pendrin and SLC26A7 were transfected in HEK293 cells (American Type Culture Collection, ATCC), assaying cellular localization or radiolabeled iodide uptake and efflux (see Methods section and supplemental appendix).

Characterization of Slc26a7-null mice. *Slc26a7*-null mice were generated as previously described (3); generation of transgenic mice expressing FLAG-epitope-tagged Slc26a7 together with their physiological, biochemical, and histological characterization is detailed in the supplemental appendix.

Statistics. Unless otherwise stated, in studies in which statistical analyses were performed, *P* values were calculated using an unpaired 2-tailed Student's *t* test and error bars represent the standard error of the mean. One-way ANOVA with a Newman-Keuls post test was used when performing multiple group comparisons, such as during the iodide supplementation study (body weight, TSH, and T4); additionally, a linear trend post test was performed in these studies. In the analysis of T3 and iodide concentrations during iodide supplementation, 2-way ANOVA with Bonferroni's post test was used. In the cellular iodide uptake study in HEK293 cells, a 1-way ANOVA with Tukey's post test was performed. *P* values less than 0.05 were considered significant and the following abbreviations were used: $*P < 0.05$, $**P < 0.005$, $***P < 0.0005$.

Study approval. All human investigations were part of an ethically approved protocol (Cambridge South, MREC 98/5/24), and/or clinically indicated, being undertaken with informed consent from patients and/or parents. All murine studies were regulated under the Animals (Scientific Procedures) Act 1986 Amendment Regulations 2012 following ethical review by the University of Cambridge Animal Welfare and Ethical Review Body (AWERB) (UK Home Office Licence no. 80/2098) or conducted in accordance to protocol 71761 approved by the University of Chicago Animal Care and Use Committee.

Author contributions

HC, AKN, and CL performed Sanger sequencing and interpretation of data. HC performed linkage analysis and EGS and NS undertook bioinformatics analysis of WES data. XHL, PS, HI, and SB performed murine studies and analyzed murine data. HC, HS, EE, OT, JK, KB, MO, JJ, KP, and TB recruited and clinically characterized patients, FEKF assisted in interpretation of clinical data. IZ generated A 7 original mice and supervised anti-FLAG immunostaining. EDW performed histological analyses. NS quantified SLC26A7 mRNA expression. ES performed cellular localization and iodide efflux studies and homology modeling and analyzed results. CAA and ERM supervised genetic studies. MS supervised murine studies. VKC, SR, and NS designed and supervised the human and murine phenotyping and functional characterization studies. The draft manuscript was written by NS; all authors contributed to discussion of the results and edited and approved the final version.

Acknowledgments

This study made use of data generated by the UK10K Project with funding from the Wellcome Trust, UK (WT091310) and we acknowledge the contribution of the UK10K Consortium. A full list of the UK10K investigators who contributed to the generation of the data is available from www.UK10K.org. This work was also supported by Wellcome Trust grants 100585/Z/12/Z (to NS) and 095564/Z/11/Z (to VKC), and the National Institute for Health Research (NIHR) Cambridge Biomedical Research Center (to VKC and NS). EGS and CAA are supported by the Wellcome Trust (098051) and EM holds an NIHR Senior Investigator Award. The University of Cambridge has received salary support with respect to EM from the NHS in the East of England through the Clinical Academic Reserve. Most studies carried out in *Slc26a7*-null mice were supported by a grant from the NIH (R37DK15070 to SR), as were XHL, PS, and HI. HC was supported by the Scientific and Technological Research Council of Turkey (TUBITAK) with grant no. 116S389.

We acknowledge the Genomics/Transcriptomics, Imaging, Histology and Disease Model Core Facilities in the Wellcome Trust-MRC Institute of Metabolic Science. The Histology Facility is supported by the UK Medical Research Council (MRC) Metabolic Disease Unit grant (MRC_MC_UU_12012/5) and the

Imaging Facility by a Wellcome Trust Strategic Award (100574/Z/12/Z); the Genomics/Transcriptomics and Disease Model Core Facilities are supported by both of these awards. Families A and B were investigated in the NIHR Wellcome Clinical Research Facility, Birmingham, and we acknowledge their expert support. We also acknowledge Lorraine Everett for her contribution to generating the FLAG-*Slc26a7* mouse model at the Wellcome Trust Sanger Institute, which was supported by the Wellcome Trust (grant 098051), and Fiona Gribble and Frank Reimann at the Wellcome Trust-MRC Institute of Metabolic Science for expert advice. The content of this article is solely the responsibility of the authors and does not necessarily represent the official views of the NHS, the Department of Health, the National Institute of Diabetes and Digestive and Kidney Diseases, or the NIH.

Address correspondence to: Nadia Schoenmakers, University of Cambridge Metabolic Research Laboratories, Wellcome Trust-MRC Institute of Metabolic Science, Level 4, Box 289, Addenbrooke's Hospital, Hills Road, Cambridge, CB2 0QQ, United Kingdom. Phone: 44.1223.767188; Email: naaa2@cam.ac.uk. Or to: Samuel Refetoff, The University of Chicago MC3090, 5841 South Maryland Avenue, Chicago, Illinois 60615, USA. Phone: +1 773.702.6939; Email refetoff@uchicago.edu.

1. Grasberger H, Refetoff S. Genetic causes of congenital hypothyroidism due to dyshormonogenesis. *Curr Opin Pediatr*. 2011;23(4):421–428.
2. Corbetta C, et al. A 7-year experience with low blood TSH cutoff levels for neonatal screening reveals an unsuspected frequency of congenital hypothyroidism (CH). *Clin Endocrinol (Oxf)*. 2009;71(5):739–745.
3. Xu J, et al. Deletion of the chloride transporter slc26a7 causes distal renal tubular acidosis and impairs gastric acid secretion. *J Biol Chem*. 2009;284(43):29470–29479.
4. Léger J, et al. European Society for Paediatric Endocrinology consensus guidelines on screening, diagnosis, and management of congenital hypothyroidism. *J Clin Endocrinol Metab*. 2014;99(2):363–384.
5. Khajavi M, Inoue K, Lupski JR. Nonsense-mediated mRNA decay modulates clinical outcome of genetic disease. *Eur J Hum Genet*. 2006;14(10):1074–1081.
6. Sharma AK, Rigby AC, Alper SL. STAS domain structure and function. *Cell Physiol Biochem*. 2011;28(3):407–422.
7. Yin K, Guo J, Lin W, Robertson SYT, Soleimani M, Paine ML. Deletion of Slc26a1 and Slc26a7 delays enamel mineralization in mice. *Front Physiol*. 2017;8:307.
8. Zou M, et al. Molecular analysis of congenital hypothyroidism in Saudi Arabia: SLC26A7 mutation is a novel defect in thyroid dyshormonogenesis. *J Clin Endocrinol Metab*. 2018;103(5):1889–1898.
9. Cavarzere P, et al. Clinical description of infants with congenital hypothyroidism and iodide organification defects. *Horm Res*. 2008;70(4):240–248.
10. Alper SL, Sharma AK. The SLC26 gene family of anion transporters and channels. *Mol Aspects Med*. 2013;34(2-3):494–515.
11. Bizhanova A, Kopp P. Controversies concerning the role of pendrin as an apical iodide transporter in thyroid follicular cells. *Cell Physiol Biochem*. 2011;28(3):485–490.
12. Twyffels L, et al. Anoctamin-1/TMEM16A is the major apical iodide channel of the thyrocyte. *Am J Physiol, Cell Physiol*. 2014;307(12):C1102–C1112.
13. Petrovic S, et al. SLC26A7: a basolateral Cl^-/HCO_3^- exchanger specific to intercalated cells of the outer medullary collecting duct. *Am J Physiol Renal Physiol*. 2004;286(1):F161–F169.
14. Petrovic S, et al. Identification of a basolateral Cl^-/HCO_3^- exchanger specific to gastric parietal cells. *Am J Physiol Gastrointest Liver Physiol*. 2003;284(6):G1093–G1103.
15. Kosiek O, et al. SLC26A7 can function as a chloride-loading mechanism in parietal cells. *Pflugers Arch*. 2007;454(6):989–998.
16. Kandasamy N, Fugazzola L, Evans M, Chatterjee K, Karet F. Life-threatening metabolic alkalosis in Pendred syndrome. *Eur J Endocrinol*. 2011;165(1):167–170.
17. Ferrandino G, Kaspari RR, Reyna-Neyra A, Boutagy NE, Sinusas AJ, Carrasco N. An extremely high dietary iodide supply forestalls severe hypothyroidism in Na^+/I^- symporter (NIS) knockout mice. *Sci Rep*. 2017;7(1):5329.
18. Pohlenz J, Rosenthal IM, Weiss RE, Jhiang SM, Burant C, Refetoff S. Congenital hypothyroidism due to mutations in the sodium/iodide symporter. Identification of a nonsense mutation producing a downstream cryptic 3′ splice site. *J Clin Invest*. 1998;101(5):1028–1035.
19. Purtell K, et al. The KCNQ1-KCNE2 K+ channel is required for adequate thyroid I^- uptake. *FASEB J*. 2012;26(8):3252–3259.
20. Tranebjærg L, Samson RA, Green GE. Jervell and Lange-Nielsen Syndrome. In: Adam MP, Ardinger HH, Pagon RA, Wallace SE, Bean LJH, Stephens K, Amemiya A, eds. *GeneReviews*. Seattle (WA): University of Washington, Seattle; 1993–2018.
21. Massart C, Hoste C, Virion A, Ruf J, Dumont JE, Van Sande J. Cell biology of H_2O_2 generation in the thyroid: investigation of the control of dual oxidases (DUOX) activity in intact ex vivo thyroid tissue and cell lines. *Mol Cell Endocrinol*. 2011;343(1–2):32–44.
22. UK10K Consortium, et al. The UK10K project identifies rare variants in health and disease. *Nature*. 2015;526(7571):82–90.
23. Kelley LA, Mezulis S, Yates CM, Wass MN, Sternberg MJ. The Phyre2 web portal for protein modeling, prediction and analysis. *Nat Protoc*. 2015;10(6):845–858.